

streak pictures. By both methods, the decay time of the measured T_i is 5 μsec . The compression field is effectively at close to peak value for about 5 μsec . The ion electron equilibration time for these structured plasmas is evidently greater than 4 μsec at 5 keV. The fast moving ($|\vec{v}| \approx 4 \times 10^5$ m/sec) ions are cooled by the cold electrons which act as field particles whose center of mass is stationary in the laboratory frame. The corresponding equilibration time for the compressed plasma is of the order of microseconds.¹⁰

This work was supported by the National Science Foundation, Grants No. GP-43733, No. PHY74-08237, and No. PHY77-07106, and the Florida Power and Light Company.

¹D. R. Wells *et al.*, Phys. Rev. Lett. **33**, 1203 (1974).

²D. R. Wells, Phys. Fluids **5**, 1016 (1962).

³D. R. Wells, J. Plasma Phys. **4**, 645 (1970).

⁴D. R. Wells and J. Norwood, Jr., Phys. Fluids **3**, 21 (1969).

⁵D. R. Wells, in *Proceedings of Third Topical Conference on Pulsed High Beta Plasmas, UKAEA Culham Laboratory, September 1975* (Pergamon, New York, 1975).

⁶D. R. Wells, Phys. Fluids **7**, 826 (1964).

⁷J. Davidson *et al.*, "The Interaction between Two Force-Free Plasma Vortices in the TRISOPS III Machine" (to be published).

⁸J. Davidson *et al.*, "Simultaneous Electron Density and Ion Temperature Measurements of a Moderately Dense Plasma Using Doppler and Stark Broadened He II Lines" (to be published).

⁹L. G. Phadke *et al.*, "A Multi-channel Monochromator for Measurement of Electron Density and Doppler Ion Temperature on the TRISOPS Facility" (to be published).

¹⁰D. J. Rose, *Plasmas and Controlled Fusion* (M.I.T. Press, Cambridge, Mass., 1961).

Observation of Stimulated Raman Backscatter from a Preformed, Underdense Plasma

R. G. Watt, R. D. Brooks, and Z. A. Pietrzyk
University of Washington, Seattle, Washington 98195
 (Received 8 May 1978)

Observations of stimulated Raman backscatter in an underdense hydrogen plasma are reported. The wavelength shift associated with the backscattered Raman component is consistent with a plasma with the measured electron density. The Raman backscatter is seen to decrease below detectable levels when the incident CO₂-laser intensity is attenuated approximately 50%, consistent with theoretical intensity thresholds of the Raman process.

The problem of parametric instabilities in plasma has been examined extensively in the literature.¹⁻⁷ Two types of solutions emerge, characterized by an infinite, homogeneous plasma¹⁻³ or finite, inhomogeneous plasma.⁴⁻⁶ In the infinite, homogeneous case, the three-wave interaction takes place throughout the entire plasma, and the applicable controlling equations can be solved to find threshold intensities and growth rates. The growth is primarily temporal but may have a spatial gain associated with it (absolute instability) in some circumstances. In the finite inhomogeneous case the interaction is treated as a local phenomenon which grows in space (convective instability). Here also in some instances there may be both spatial and temporal growth. Both approaches predict a number of different instabilities. The decay of an incident photon into a backscattered photon and an ion-

acoustic wave [stimulated Brillouin scattering (SBS)] has been observed in numerous experiments, primarily in Nd:glass-laser-heated solid targets^{8,9} and in CO₂-laser-heated linear devices.¹⁰⁻¹² Decay of an incident photon into two electron plasma waves (two-plasmon decay mode)¹³ or into one electron-plasma wave and one ion-acoustic wave (parametric decay mode)¹⁴ have also been observed. The observation reported here is the decay of an incident photon into a backscattered photon and an electron plasma wave [stimulated Raman scattering (SRS)]. Stimulated Raman backscatter is characterized by an exponential backscattered-intensity dependence on the incident intensity and a backscattered frequency which is shifted to a lower frequency than the incident frequency by the electron plasma frequency $\omega_p = (e^2 n_e / \epsilon_0 m_e)^{1/2}$. Possible indirect evidence of the Raman process has been reported in the liter-

ature¹⁵ in the form of observed backscattered radiation at $\frac{3}{2}\omega_0$ which could be produced near a quarter-critical surface ($\frac{1}{2}\omega_0 = \omega_{pe}$) but to our knowledge this is the first direct spectral evidence of SRS.

The apparatus used in the experiment is diagrammed in Fig. 1. A 20-cm long, 4-cm-diam, 16.5-kG θ pinch is used to create and confine the plasma. A transverse-excitation atmosphere CO₂ laser capable of focused intensities of approximately 3×10^9 W/cm² and associated salt optical system provides additional heating. Axial double-pulse holography was used to characterize the density profiles of the plasma in the absence of laser heating (not shown on schematic). A ruby-laser Thomson-scattering system incorporating a 6-J, 30-ns oscillator-amplifier chain, a tandem monochromator ($\frac{1}{4}$ m Jarrell-Ash), and an extended-response optical multichannel analyzer (PARC 1205I) provides diagnostics for the laser-heated plasma. An ir spectrometer is used for analysis of the backscattered light. Thomson scattering is also used to evaluate the multiple-

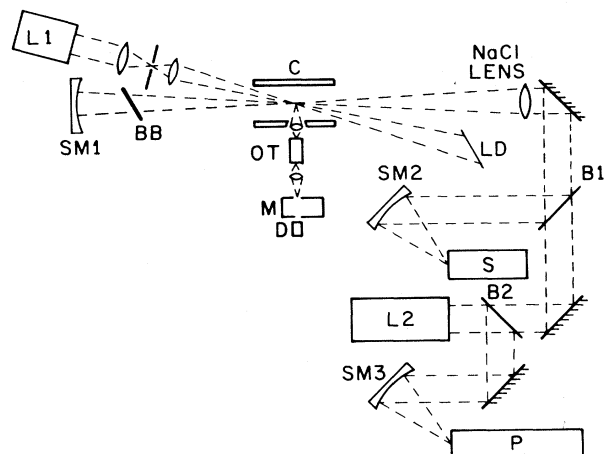


FIG. 1. Experimental configuration. The plasma is formed in a single-turn solenoid (C), and heated by a transverse-excitation atmosphere CO₂ laser (L2) and multiple-passing optical train utilizing a spherical focusing mirror (SM1) and sodium chloride lens. Plasma diagnostics are provided by a ruby laser (L1), fiber-optic collection system (OT), and $\frac{1}{4}$ -m monochromator (M) observed by a silicon intensified target 500-channel optical analyzer (D). The incident CO₂ beam is monitored by a beam splitter (B2), spherical mirror (SM3) and photon-drag detector (P). The red-shifted Raman radiation is beam split off (B1) and sent via focusing mirror (SM2) to the ir spectrometer (S). There is a polycarbonate CO₂ beam dump (BB) in the CO₂ optical train allowing operation in either single- or multiple-pass mode.

pass heating experiment being run concurrently on the system. Results of that work will appear in a later publication.

The plasma parameters at the time of the Raman scattering measurements are $n_e = (2 \pm 0.5) \times 10^{16}$ cm⁻³ and $T_e = 15 \pm 5$ eV, resulting from single-pass heating. The measurements reported are spectra for single-ended illumination of the plasma, an option which allows a much less ambiguous interpretation of the processes involved than would the double-ended illumination existing in the multiple-pass mode of operation.

In order to provide direct evidence of the presence of a stimulated process we measured the overall backscattered intensity as a function of incident intensity using a pyroelectric detector with a sensitivity of 0.005 V/W and a risetime of 5 ns. If the backscatter increases linearly with incident intensity, then one may interpret it as either reflections from optical components or as Thomson-scattered CO₂ radiation. If, on the other hand, the radiation varies exponentially with the incident intensity, then it can be interpreted as arising from some nonlinear process. The results shown in Fig. 2 clearly indicate the exponential behavior of the backscattered radiation. It should be noted that no wavelength dispersion was involved for this data, so that both SRS and SBS may be present. When the intensity of the incident radiation was reduced below about 3×10^8 W/cm², the backscattered signal fell below detectable lim-

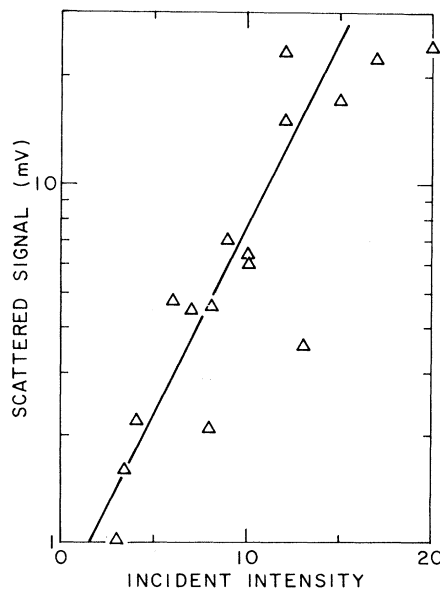


FIG. 2. Measured backscattered-signal amplitude as a function of incident CO₂ intensity.

its with the pyroelectric detector. The detector signal was about 10 W at its largest, implying a reflectivity of approximately 10^{-5} for the combined SRS and SBS backscatter.

Since both SRS and SBS processes may be occurring in our plasma (the infinite homogeneous threshold intensity for SBS is approximately 6×10^6 W/cm²; that for SRS is approximately 4×10^7 W/cm²), it was necessary to disperse spectrally the backscattered radiation. The resulting spectra (for large wavelength shifts) is shown in Fig. 3. This spectrum was the result of a shot-to-shot scan utilizing the ir spectrometer with a (Hg-Cd)Te detector having specific detectivity $D^* = 1.3 \times 10^{10}$ cm² Hz^{-1/2}/W, giving a sensitivity of 0.4 mV/ μ W into 50 Ω . Typical oscilloscope traces are shown in Fig. 4. The peak of the spectra, if interpreted as the plasma frequency, corresponds to 1.5×10^{16} cm⁻³ in good agreement with the other diagnostics. Vacuum shots show no scattered radiation at the 11- μ m peak of the Raman spectra. It should be noted that allowing for the geometry of the detector and the efficiency of the spectrometer, the Thomson-scattered CO₂ signal at 11 μ m would yield only a 4×10^{-10} -W signal at the detector whereas the measured spectra peaked at over 4 μ W, so that $I_{\text{Raman}} \approx 10^4 I_{\text{thermal}}$.

Finally we attempted to check the exponential dependence of the 11- μ m light by attenuating the incident beam and examining the resultant backscattered light at the spectrometer exit plane. It was found that when the incident intensity was decreased below about 60% of its peak (3×10^9 W/cm²) the scattered signal dropped below the noise level (~ 4 mV) and became undetectable. The decrease is definitely nonlinear and appears to be stronger than exponential, which suggests a threshold behavior.

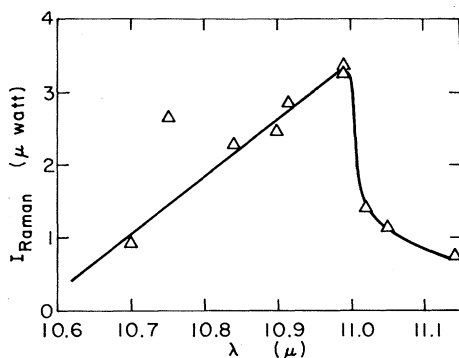


FIG. 3. Backscattered spectrum as a function of wavelength.

We interpret the data from the total-backscattered-intensity scan as a clear indication of the presence of nonlinear processes such as SRS and SBS. The spectrally resolved backscatter has a shape very consistent with the theoretical growth-rate curves,² although the value of $k_0 \lambda_D = 0.16$ measured via Thomson scattering is a bit low to explain the width of the observed spectra. There are two possible causes for this discrepancy. First, the theoretical curves were calculated based only on Landau damping of the plasma wave, whereas in this plasma both Landau damping and collisional damping are present and comparable, which would tend to broaden the curves. Second, the parabolic density profile present in the plasma may allow more than one density regime to contribute to the SRS, and the superposition of the

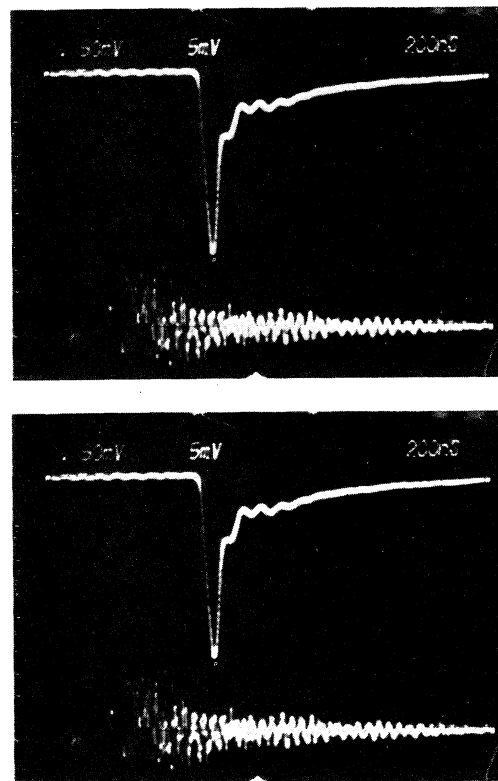


FIG. 4. Typical oscilloscope traces. The upper trace in each case is the incident-photon-drag detector signal, showing the time history of the incident intensity (200 ns/cm). The full width at half-maximum of the spike is approximately 70 ns. The lower trace in the top photograph is the response of the (Hg-Cd)Te detector looking at the 11- μ m output of the ir spectrometer with no plasma present. The lower trace in the bottom photograph is the signal at 11 μ m with the plasma present.

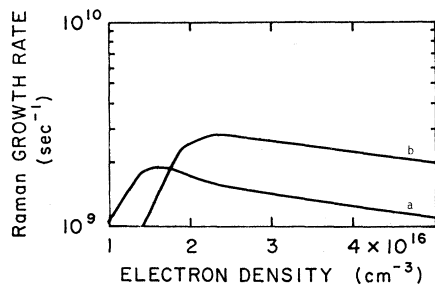


FIG. 5. Theoretical growth rates for SRS as a function of density. The growth rates were calculated for (a) a 10-eV and (b) 15-eV hydrogen plasma, in the infinite homogeneous case.

various backscattered spectra would also cause a broadening of the observed spectra in the lower-wavelength region.

A question arises as to why we were able to observe SRS when other attempts have failed. We believe the reasons are the following. Our plasma, which is 20 cm long, has a much larger absorption length for CO₂ radiation (~1000 cm) than its length so the CO₂ radiation does not create severe temperature and density gradients. Furthermore, the preformed plasma is very homogeneous axially (as well as having a smoothly varying density profile capable of containing the beam for the entire plasma length). Consequently conditions are favorable for high growth rates and for the measured laser intensity, the plasma lies on a maximum in the growth rate between regions dominated by collisional damping ($n_e > 10^{17}$ cm⁻³, 10 eV) and electron Landau damping ($n_e < 10^{16}$, 10 eV) (Fig. 5). The high growth rate allows the SRS to grow to detectable levels during the period while the laser intensity is well above threshold. A search for SRS in the University of Washington slow solenoid apparatus¹⁰ was not successful. This device operates in a breakdown mode with very short absorption lengths and steep gradients. The temporal growth rate is smaller than in the infinite homogeneous case and the instability depends on a length of plasma large enough for the backscatter to build to detectable levels,

which may not have existed. In solid targets the breakdown nature of the plasma generates severe density gradients. Since SRS depends on frequency ($\omega_0 = \omega_R + \omega_p$) and wave-number ($\vec{k}_0 = \vec{k}_R + \vec{k}_p$) matching (as must all three-wave interactions) and since $\omega_p \sim \omega_{pe} = (e^2 n_e / \epsilon_0 m_e)^{1/2}$, any density gradients will lead to a frequency mismatch in a short distance prohibiting buildup of the waves.

This work was supported by the National Science Foundation.

¹M. V. Goldman and D. F. DuBois, *Phys. Fluids* **8**, 1404 (1965).

²J. Drake, P. K. Kant, Y. C. Lee, G. Schmidt, C. S. Liu, and M. N. Rosenbluth, *Phys. Fluids* **17**, 778 (1974).

³K. Nishikawa, *J. Phys. Soc. Jpn.* **24**, 916, 1152 (1968).

⁴D. W. Forslund, J. M. Kindel, and E. L. Lindman, *Phys. Fluids* **18**, 1002 (1975).

⁵D. W. Forslund, J. M. Kindel, and E. L. Lindman, *Phys. Rev. Lett.* **30**, 739 (1973).

⁶C. S. Liu, M. N. Rosenbluth, and R. B. White, *Phys. Rev. Lett.* **31**, 697 (1973).

⁷V. N. Tsytovich, *Nonlinear Effects in Plasma* (Plenum, New York, 1970).

⁸C. Yamanaka, T. Yamanaka, T. Sasaki, and J. Mizui, *Phys. Rev. Lett.* **32**, 1038 (1974).

⁹B. H. Ripin, J. M. McMahon, E. A. McLean, W. M. Manheimer, and J. A. Stamper, *Phys. Rev. Lett.* **33**, 634 (1974).

¹⁰R. S. Massey, K. Berggren, and Z. A. Pietrzyk, *Phys. Rev. Lett.* **36**, 963 (1976).

¹¹John J. Turechek and Francis F. Chen, *Phys. Rev. Lett.* **36**, 720 (1976).

¹²A. A. Offenberger, M. R. Cervenak, and P. R. Smy, *J. Appl. Phys.* **47**, 1451 (1976).

¹³J. J. Schuss, T. K. Chu, and L. C. Johnson, *Phys. Rev. Lett.* **40**, 27 (1978).

¹⁴A. Y. Wong *et al.*, in *Proceedings of the Fourth International Conference on Plasma Physics and Controlled Thermonuclear Fusion Research, Madison, Wisconsin, 1971* (International Atomic Energy Agency, Vienna, Austria, 1971), Vol. I, p. 335.

¹⁵N. H. Burnett, H. A. Baldis, G. D. Enright, M. C. Richardson, and P. B. Corkum, *J. Appl. Phys.* **48**, 3727 (1977).

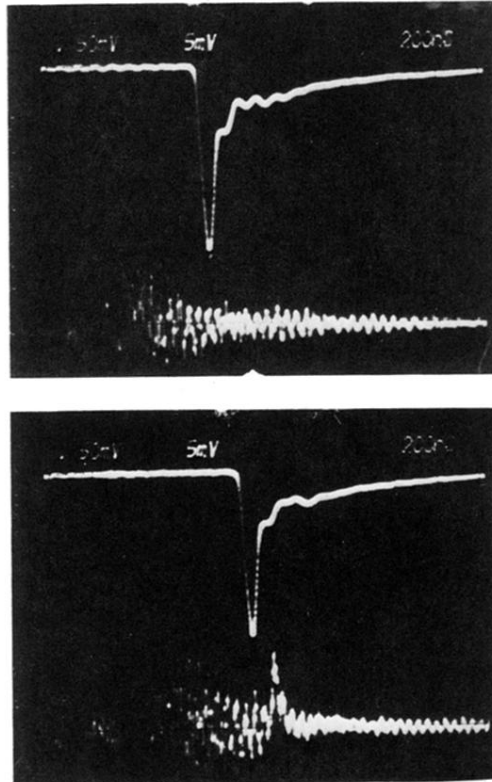


FIG. 4. Typical oscilloscope traces. The upper trace in each case is the incident-photon-drag detector signal, showing the time history of the incident intensity (200 ns/cm). The full width at half-maximum of the spike is approximately 70 ns. The lower trace in the top photograph is the response of the (Hg-Cd)Te detector looking at the 11- μm output of the ir spectrometer with no plasma present. The lower trace in the bottom photograph is the signal at 11 μm with the plasma present.